

High performance dual-mode flexible surface acoustic wave resonators for UV light sensing

Xing-Li He, Jian Zhou, Wen-Bo Wang, Wei-Peng Xuan, Hao Jin and Ji-Kui Luo

Abstract—Dual-mode flexible ZnO/polyimide surface acoustic wave (SAW) based ultraviolet (UV) light sensors were fabricated and their performances were investigated. UV light sensing measurements showed that the responses of the dual wave modes of the sensors increase with the increase of light intensity and the frequency changes linearly with the change of light intensity. Under a 4.5 mW/cm² UV light illumination, the resonant frequency of the Rayleigh wave decreased up to ~43 kHz, while that of the Lamb wave was approximately 76 kHz. The UV light sensitivities for the two resonant modes are 111.3 and 55.8 ppm/(mW/cm²), respectively. The resonant frequency, phase angle and amplitude of the two resonant modes exhibited a good repeatability in responding to cyclic change of the UV light, and an excellent stability up to a long duration of UV light exposure. The dual-mode flexible SAW resonators are simple in structure, more accurate in detection, and can be fabricated at low cost, therefore are very promising for application in flexible sensors and electronics.

Index Terms—Flexible SAW, ZnO/Polyimide, UV sensor

I. INTRODUCTION

OWING To their unique properties such as flexibility, light-weight and low cost [1], flexible electronics have been regarded as one of the top ten emerging technologies in the 21st Century, and have been intensively studied. Great efforts have been made to develop a number of flexible electronics such as field effect transistors [2], integrated circuits [3] eyeball cameras [4], memory [5], nanogenerator [6] and photodetector [7],[8] etc. However, the lack of high performance flexible radio frequency (RF) resonators severely

restricts the development of sensing and monitoring systems using flexible electronics, especially the remote, wireless and passive sensing network. Surface acoustic wave (SAW) resonators are a type of high frequency RF resonators, and are essential devices for the development of many systems for sensing physical variables as well as biochemical substances, especially the wireless and passive sensing systems. SAW devices are also one of the building blocks for electronics, communication, microsensors and microsystems. Recently, our research group has successfully developed ZnO/Polyimide based flexible SAW devices [9],[10]. These flexible SAW devices showed high performance for electronic applications, and they can also be used as the temperature and humidity sensors with high sensitivities, and as microactuators to pump liquids in small volumes with a velocity up to 34 mm/s and to concentrate nanoparticles in a few seconds, demonstrated their very promising applications in communication, sensing, microfluidics and lab-on-chips (LOC).

ZnO is a semiconductor with an energy band gap of ~3.3 eV, able to absorb ultraviolet (UV) light, and has been widely used to develop UV-light detectors [11]-[14]. Owing to the advantages of high sensitivity, low-cost, high reliability and good reproducibility of SAW devices, many ZnO-based SAW UV light sensors have been developed, and their structures and performances have been studied [11]-[14]. Most of the SAW UV light sensors reported use the Rayleigh-wave mode to detect the acoustic-electric interaction, and limited work has been done to investigate the responses of other wave modes of the SAW devices to UV light. Pang et al reported Love wave-based SAW UV light sensors using a ZnO film deposited on a 36° Y-cut LiTaO₃ substrate [15], showed a large frequency shift of about 150 kHz under a 254 nm light illumination with a light intensity of 350 μW/cm². Wang et al studied the response of a thin film ZnO-based Lamb wave sensor to UV light, and demonstrated an insertion loss increase of 1.8 dB at a low intensity of a 370 nm light illumination [16]. Although a lot of ZnO-based SAW UV light sensors have been developed and studied, all of them had a single wave mode. This restricts the sensing accuracy and/or requires a complicated calibration circuit and sensors for temperature etc in practical applications. Furthermore, all of them were made on rigid substrates, thus they are expensive and not suitable for flexible electronic applications. Here we report on the development of first flexible SAW-based UV-light detector with high sensitivity, and show that the devices have dual wave modes and both of them are highly sensitive to the UV light. We also show all the

This work was supported by the National Natural Science Foundation of China (No. 61171038, 61204124, 61274037), the Zhejiang Province Natural Science Fund key Project (No.J20110271), and the Zhejiang Provincial Natural Science Foundation of China (No. LQ12F01007, Z11101168). The authors also would like to acknowledge the financial support by the Innovation Platform of Micro/Nanodevices and Integration System, Zhejiang University.

X.-L. He, J. Zhou, W.-B. Wang, W.-P. Xuan, and H. Jin and are with the Department of Information Science & Electronic Engineering, Zhejiang University and Cyrus Tang Center for Sensor Materials and Applications, 38 Zheda Road, Hangzhou 310027, China.(e-mail: hexingli@zju.edu.cn; 11031028@zju.edu.cn; iseelisa@zju.edu.cn; 11231014@zju.edu.cn; hjin@zju.edu.cn)

J.-K. Luo is with Institute of Renewable Energy and Environment Technology, University of Bolton, Deane Road, Bolton, BL3 5AB, United Kingdom.(e-mail:J.Luo@bolton.ac.uk)

transmission variables (resonant frequency, phase angle and insertion loss) of the devices can be used for the detection of UV light changes simultaneously, greatly enhance the sensing accuracy.

II. EXPERIMENTAL DETAILS

A. Thin film deposition

Kapton polyimide (PI) films were used as the substrates for the deposition of ZnO piezoelectric (PE) thin films and the fabrication of the flexible SAW devices as they can withstand high temperatures up to 300 °C and have a smooth surface [17] which allows the deposition of high quality PE ZnO films. Direct-current (DC) reactive magnetron sputtering was used to deposit the ZnO films on the polyimide substrates. The ZnO target has a purity of 99.99% and a diameter of 100mm. The distance between the substrate and the target was fixed at 70 mm. An Ar/O₂ gas mixture with a ratio of 100/50 (sccm) was used for the deposition. The deposition conditions have been optimized with details reported in ref.[18], and have been used here for the deposition of the ZnO films without further optimization. The substrate temperature, DC power, deposition pressure and bias voltage were 200 °C, 200 W, 2.0 Pa and 75 V, respectively. The ZnO film thickness is ~4 μm for all the devices used in this study. The relevant deposition and characterization results can be found from our previous works [9],[18].

B. Material characterization

The crystal structure and surface morphology of the ZnO thin films were characterized by scanning electron microscopy (SEM) (S4800, Hitachi), x-ray diffraction (XRD) (XRD-6000, Shimadzu) and atomic force microscopy (AFM) (SPI-3800N, Seiko). Photoluminescence (PL) measurement was used to characterize the optical property of the ZnO films as these strongly affect the photo-carrier generation [15],[19],[20]. A fluorescence spectrophotometer (FLS-920, Edinburgh Instruments) excitation of 325 nm was used for the measurement at room temperature (~26 °C).

C. SAW device fabrication and characterization

Polyimide layers are normally used as an acoustic absorber because of the low acoustic impedance [21],[22]. The softness of the substrate will degrade the transmission property of the SAW devices made on the polyimide substrates. SAW devices with shorter wavelengths therefore, are desirable as more percentage of the surface acoustic waves will locate in the ZnO layer rather than in the PI substrate that can improve the performance of the SAW devices. The wavelength, λ , of the SAW devices was then set to be 20 μm for this work. The aperture is 4000 μm, and the SAW devices have 20 pairs of interdigitated transducers (IDTs), with 10 pairs of reflective grating. The distance between the receiver and the transmitter was fixed at 20λ . A standard UV-light photolithography and lift-off process were employed to fabricate the flexible SAW resonators. An aluminum (Al) layer with a thickness of ~80 nm was used for the IDTs, which was deposited by thermal

evaporation. Figure 1(a) is a schematic drawing of the flexible SAW devices and 1(b) is a microphoto of the fabricated SAW devices on a polyimide film used for the UV light detection. The transmission and reflection characteristics of the SAW devices were measured using an Agilent E5071C network analyzer.

Numerical analysis of the resonators was carried out by using COMSOL Multiphysics® (Comsol Ltd). A simplified model with ideal material parameters and infinite periodic boundary conditions was used.

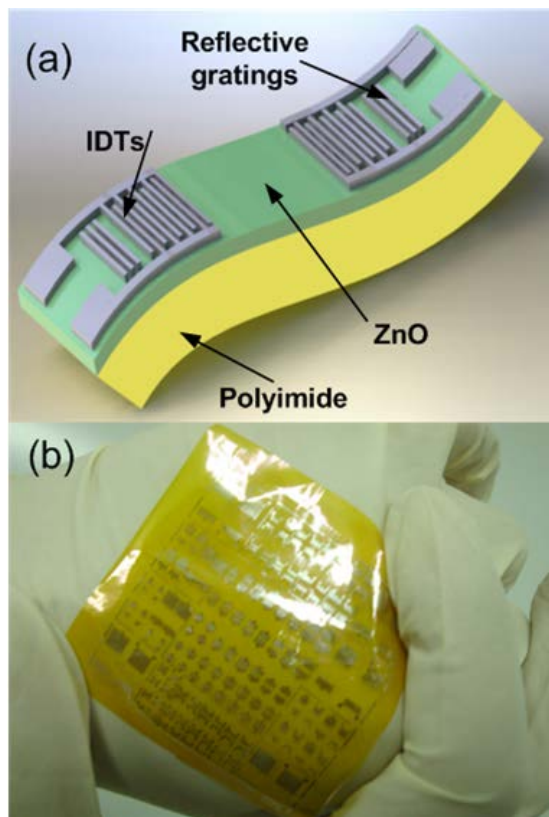


Fig. 1. A 3D schematic drawing of the flexible SAW device (a), and a photo of the fabricated flexible SAW devices on a polyimide film (b), which has many SAW devices with different designs.

D. UV-light sensing

The response of the sensors to UV light illumination was investigated by measuring the changes of the transmission characteristics of the flexible SAW resonators. The UV light has a fixed wavelength of 365 nm. A UV lamp (ANUP 5252, Panasonic) was used to generate the UV light, and a 365 nm monochromator was used to filter the UV light. A LabVIEW (National Instrument) based program was developed to implement the automated measurements to record the parameter changes with time. A schematic view of the testing system is shown in figure 2. All device characterization and UV light detection were conducted at room temperature. The temperature was monitored during UV light exposure, no significant temperature rise was observed.

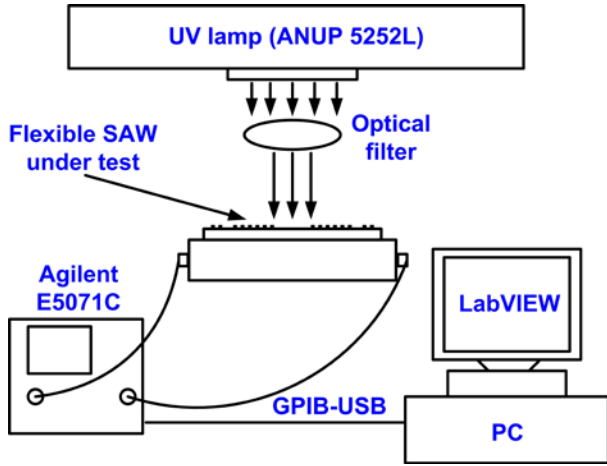


Fig. 2. A schematic view of the testing system used for the UV light detection.

III. RESULTS AND DISCUSSIONS

Figure 3 shows the transmission spectrum (S_{21}) and the corresponding phase angle of a SAW device. The device resonates at 75.7 MHz and 254.3 MHz respectively, corresponding to the Rayleigh wave and Lamb wave. The signal amplitudes of both the wave modes are about 20 dB, showing high performance. The quality factors of the two wave modes are 31 and 57 respectively, calculated by a -3dB method [23].

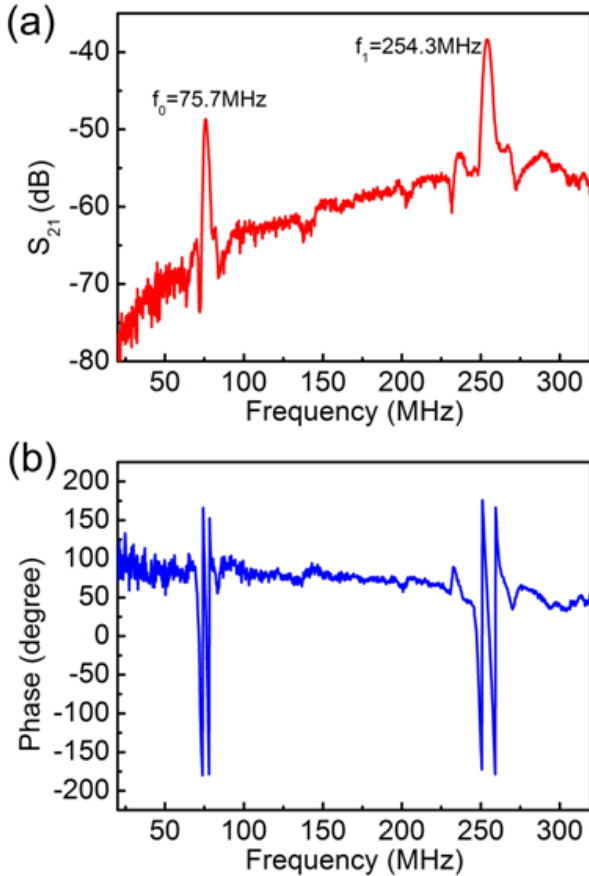


Fig. 3. Transmission spectrum (a) and relevant phase angle (b) of a ZnO/PI based dual-mode SAW resonator. The wavelength of the resonator is 20 μ m.

The effective electromechanical coupling coefficients (k^2) of the devices were calculated by the following equation [24],

$$k^2 = \frac{\pi G_m(f_r)}{4NB_s(f_r)} \quad (1)$$

where N is the finger pairs, $G_m(f_r)$ and $B_s(f_r)$ are the motional conductance and static susceptance at the resonant frequency f_r , respectively. The k^2 were found to be $\sim 0.35\%$ and $\sim 0.71\%$, for the Rayleigh and Lamb modes of the devices respectively, compatible to those made on rigid Si-substrates [25],[26].

Figure 4(a) is the comparison of the measured reflection spectrum with the simulated one, showing a good agreement with each other, and the two modes are therefore, indeed the Rayleigh and Lamb waves. Figure 4(b) is the deformation of the resonator at ~ 76 MHz. It can be seen that the deformation penetrates into the polyimide substrate, but the largest deformation is within the ZnO film near the surface as indicated by the red-colored part, implying the acoustic energy is largely confined within about one wavelength near the surface. The deformation is an asymmetric resonance, corresponding to the Rayleigh mode. The deformation of the device at ~ 260 MHz is shown in figure 4(c). The shape of the resonator is similar to that of conventional symmetric Lamb wave, and is a symmetric deformation over the substrate. This resonant mode represents the Lamb wave mode.

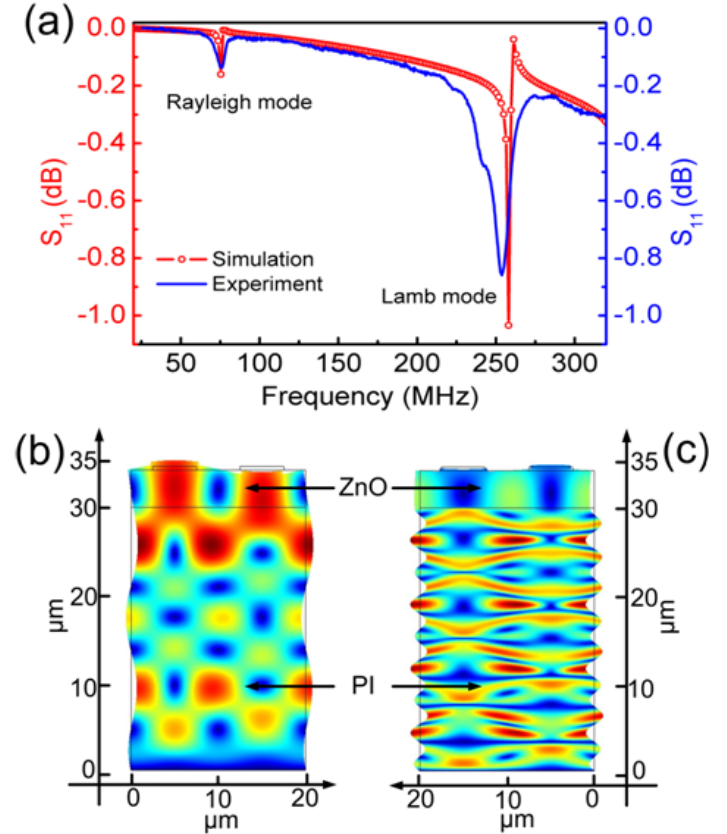


Fig. 4. (a) Comparison of a typical reflection spectrum (blue line) of the SAW resonators with the simulated spectrum (red line). A cross sectional view of the resonator deformation at resonance for (b) Rayleigh mode and (c) Lamb mode.

The simulated frequency of 260 MHz of the Lamb wave is larger than 254.3 MHz of the experimental one. The difference between the experimental and simulated results is attributed to the use of the simplified model and ideal material parameters in the modeling, and it is expected that the deviation increases with increase in frequency. The material properties of a single crystalline ZnO film were used in modeling, while the practical ZnO films were polycrystalline obtained by sputtering deposition, which also have high densities of structure defects and impurities. These defects in the ZnO films will deteriorate the performance of the devices, resulting in a lower resonant frequency and smaller signal amplitude compared with the ideal case of the single crystalline ZnO material.

The changes of the resonant frequency, phase angle and insertion loss of the two wave modes under different UV intensities have been investigated with the results shown in figures 5(a) - 5(f). The frequency shifts of the two resonances

increase with the increase in UV light intensity. For the Rayleigh wave, the frequency shifted downward by ~ 6 kHz when the UV light intensity was 0.4 mW/cm^2 , and increased to ~ 43 kHz under a 4.5 mW/cm^2 illumination. For the Lamb resonance, the frequency shift also increased when the UV light intensity was increased, and a maximum shift of 76 kHz was obtained under a 4.5 mW/cm^2 UV light illumination. The phase angles of the two resonant modes also changed simultaneously with the increase in UV intensity. A maximum phase shift of $\sim 2.1^\circ$ and $\sim 2.4^\circ$ were obtained for the Rayleigh wave and Lamb wave, respectively, as shown in figures 5(c) and 5(d). On the other hand, the amplitude of the transmission signal of the two modes increased (the insertion loss decreases) with the increase in UV light intensity, different from what normally observed.

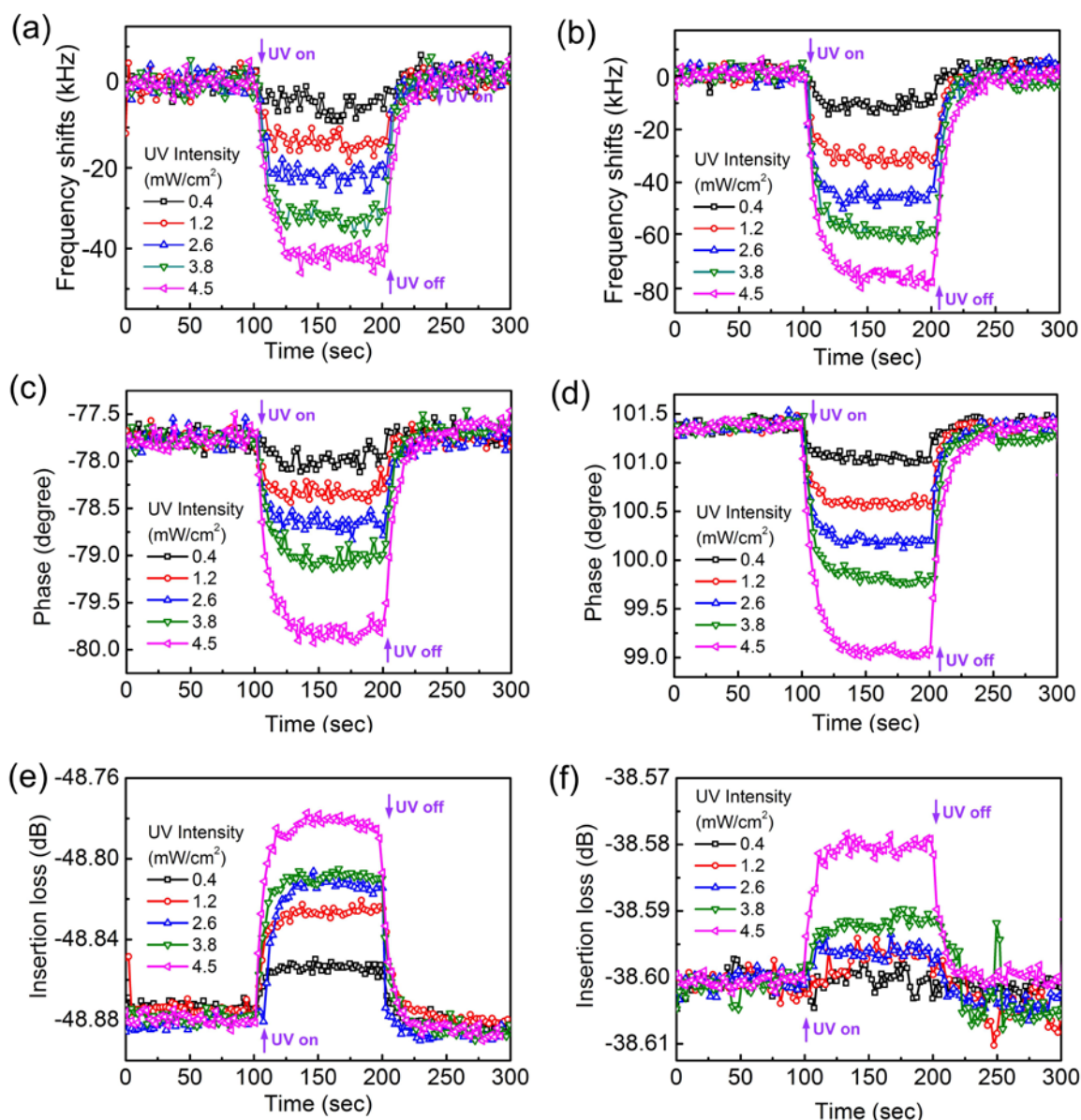


Fig. 5. Frequency responses of flexible SAW sensor under UV light illumination with different power intensities for the Rayleigh mode (a) and Lamb mode (b). Phase responses of the Rayleigh mode (c) and Lamb mode (d) waves. Insertion loss changes of the Rayleigh (e) and Lamb (f) mode.

But the insertion loss changes are very small, in the order of about 0.1dB, much smaller compared with those (over 10 dB) reported by Pang et al [15], probably due to the different structures used.

The UV light response of the ZnO SAW sensors is mainly attributed to the photo-generated free carriers which change the conductivity of the surface layer of the device. When the UV light is exposed to the ZnO, electrons in the valance band are emitted into the conduction band, leading to the generation of free electron-hole pairs. The absorption coefficient of the ZnO at 365 nm light is about $10^4 \sim 10^5 \text{ cm}^{-1}$ [27], therefore the photo-generated carriers are confined to the surface layer of the ZnO film. The free carriers will interact with the surface acoustic field, resulting in a change in the transmission characteristics. The surface sheet conductivity can be expressed as $\sigma_s = \nu_0 C_s$, where C_s and ν_0 are the capacitance per unit length and the original phase velocity of the surface acoustic wave respectively [15],[28]. The velocity shift (Δv) of the surface and the attenuation (insertion loss) Γ are determined by the following equations [12],[15],[28],

$$\frac{\Delta v}{\nu_0} = -\frac{k^2}{2} \frac{1}{1 + (\sigma_s / \sigma_M)^2} \quad (2)$$

$$\Gamma = \frac{k^2}{2} \frac{2\pi}{\lambda} \frac{\sigma_s \sigma_M}{\sigma_s^2 + \sigma_M^2} \quad (3)$$

where σ_M and λ are the material property (the relaxation conductivity) and wavelength, respectively. Eq.(2) implies that a change of surface conductivity will result in a decrease of the propagation phase velocity which in turn changes the resonant frequency as they are correlated by $f_r = (\nu_0 + \Delta v) / \lambda$. The change of the phase angle is induced by the variation in the phase velocity, and is given by [29],[30]

$$\Delta \phi = \frac{\Delta v}{\nu_0} \frac{2\pi L}{\lambda} \quad (4)$$

where L is the length of the acoustic path between the two IDTs of the resonators. As indicated by eq.(3), a change of the surface conductivity and capacitance will influence the insertion loss of the transmission. The insertion loss normally increases (i.e. the signal amplitude decreases) under a UV light illumination [12],[15],[20]. However, the insertion loss of both the wave modes of our devices was found to decrease (the signal amplitude increases) under light illumination though the change is very small ($< 0.1\text{dB}$), different from what is normally observed and expected. Although such a phenomenon was observed for the third harmonic Rayleigh wave of ZnO/Si based UV sensors [20], the reason is still not clear, and needs further investigation. A possible explanation for our flexible sensors is the stress relaxation of the ZnO/polyimide bimorph structure under light illumination (optothermal effect), the SAW devices perform better, and the signal amplitudes become larger, which is reversible when the light is switched off,

consistent with the results obtained.

for acoustic wave devices based on ZnO or AlN, the resonant frequency of the devices is expected to change linearly with the light intensity, and is attributed to the change of the photo-generated carrier concentration linearly with light intensity [14],[15],[31],[32]. As shown in figure 6(a), the frequency shifts of both the Rayleigh and Lamb modes indeed increase linearly with the increase in light intensity, in agreement with the theoretical analysis. Eq.(2) and eq.(4) also imply that the change of the phase would be a linear function of light intensity as well, similar to that of the resonant frequency, and it is indeed the case as shown in figure 6(b). Similarly, the insertion loss decreases linearly with the increase in light intensity for both the Rayleigh and Lamb modes as shown in

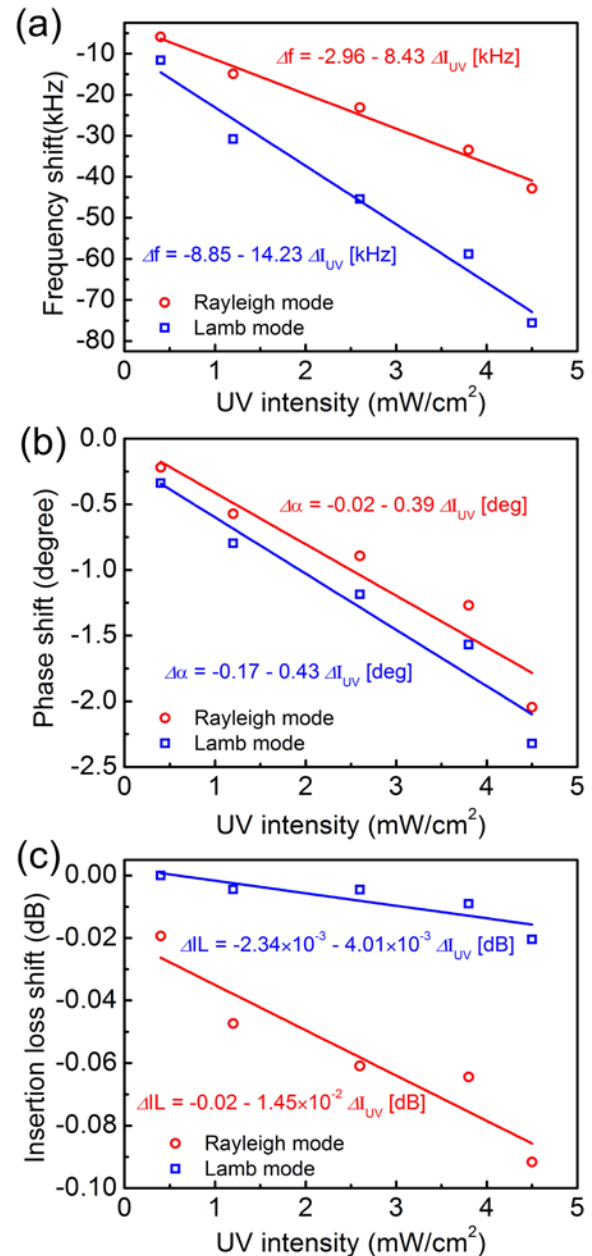


Fig. 6. Resonant frequency (a), phase angle (b) and insertion loss (c) shift as a function of UV intensity for flexible SAW sensors, showing different UV

sensitivities for Rayleigh and Lamb mode.

figure 6(c). The UV light sensitivity of the SAW devices is defined as [14],

$$S_{UV} = \frac{1}{f_r} \frac{\Delta f}{\Delta I_{UV}} \quad (5)$$

Where Δf and ΔI_{UV} are the frequency shift and the variation of the light intensity, respectively. The UV light sensitivity for the Rayleigh wave is 111.3 ppm/(mW/cm²), while that is 55.8 ppm/(mW/cm²) for the Lamb mode wave, even though the latter has a larger frequency shift under the same light illumination. The sensitivity of the Rayleigh mode is close to the value of 114.9 ppm/(mW/cm²) reported by Sharma et al [12], while the sensitivity of the Lamb wave of the flexible SAW devices are much larger than those reported in ref.[16], where the resonant frequency barely changed when illuminated by a 0.5 mW/cm² 370 nm light. The results demonstrate that the flexible SAW UV light detectors have compatible or better sensitivities to those on rigid substrates, and have great potential for applications.

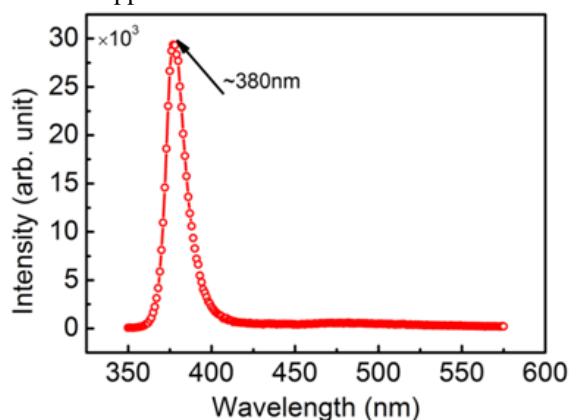


Fig. 7. A typical PL spectrum of the ZnO films on a PI substrate. The thickness of the ZnO film is $\sim 4 \mu\text{m}$. It shows a single large peak round at 380nm, corresponding to the band-to-band emission.

The high UV sensitivities of both the wave modes of the flexible SAW sensors are attributed to the excellent crystal quality and optical properties of the ZnO film obtained. The ZnO crystals films deposited on the polyimide substrates have a highly c-axis orientation and large grain size as shown by the SEM and XRD characterization in our previous papers [9],[18]. The ZnO films deposited on the polyimide substrate also showed a strong PL emission as shown in figure 7. The strong peak around 380nm wavelength corresponds to the electron transition from the localized level slightly below the conduction band to the valence band of ZnO [33]. The emissions from defects such as oxygen vacancies and zinc interstitials are typically round 450~500 nm [34],[35], but they are very weak in our samples, indicating that ZnO films on the PI substrates have very good crystallinity and optical property, and very low defect densities. These greatly enhance the absorption of the UV light and photo-carrier generation, resulting in a strong response to the UV light and a high

sensitivity of the sensors. The reason for why ZnO films on PI substrate exhibited such high quality is still under investigating. A possible explanation is that, comparing with the ZnO film on rigid substrate, PI substrate is easier to release the stress which was introduced by sputtering, which equals to a thermal annealing process. In order to better understanding the mechanism, more work need to be done.

The repeatability and stability of the flexible SAW UV light sensors have been investigated. Figure 8(a) shows the cyclic response of the resonant frequencies of the SAW sensor when it was illuminated cyclically with a 4.5 mW/cm² intensity. The resonant frequencies decrease rapidly when the UV light was switched on, and saturate after a transient time. The frequency response times for both the waves are about 10~12 s, comparable to the results reported by others [15],[31]. The maximum shifts of the frequencies of the Rayleigh and Lamb waves remain at $\sim 43 \text{ kHz}$ and $\sim 76 \text{ kHz}$, respectively, unchanged with the time and repeated illumination, showing its

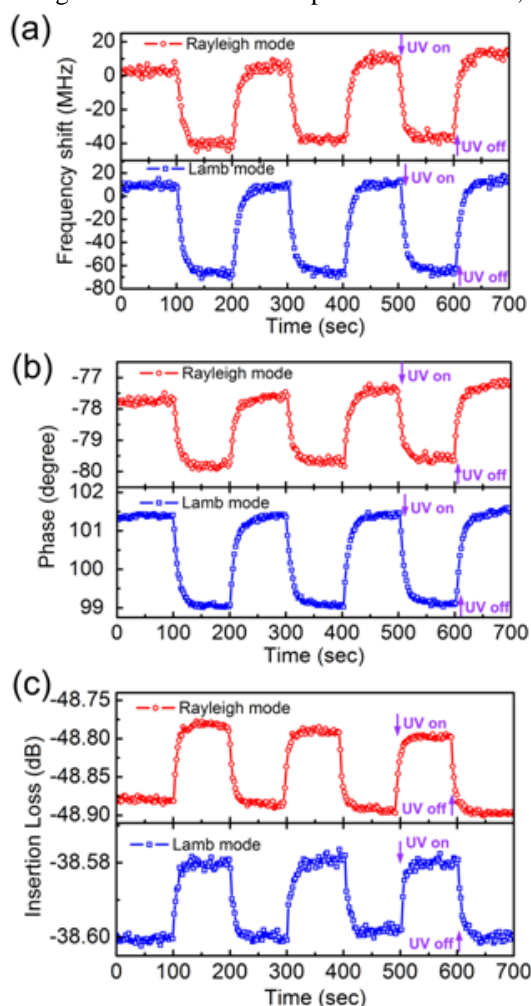


Fig. 8. Response of the flexible SAW sensor to a cyclic illumination of the UV light: Responses of resonant frequency (a), phase (b) and insertion loss (c). The UV light intensity is 4.5 mW/cm².

good stability. When the UV light was switched off, the resonant frequencies of both the wave modes return to the original values, and the recovery times are slightly longer than the rising times for both the modes. Similarly, under the UV

light illumination, the phases (figure 8(b)) of the two modes changed in the same way as the change of the resonant frequencies, while the signal amplitude (figure 8(c)) of both the resonant modes shifted in the opposite direction (i.e. increased) simultaneously.

All the variables of the two wave modes show a completed recovery to their original values without any deterioration after three times repeated illumination of the UV light, showing the excellent repeatability and stability of the dual-mode flexible SAW sensors. To test the stability over a very long, the transmission properties of the devices after a UV light illumination up to 60 min were investigated. Shown in figure 9(a), for Rayleigh mode, when the temperature was almost constant ($\pm 0.2^\circ\text{C}$), the frequency change was constant, and no any degradation of the transmission properties of the sensors was observed, when the UV light was turn off, the resonant frequency of the sensors would recover to the original value. The simultaneously influences of both UV light and temperature were also investigated (figure 9(b)), the sensors were tested in a closed room, within which the temperature was controlled by an air conditioning. Since these sensors possess negative TCF [9], the resonant frequency changed oppositely to the changed of temperature. When the sensors were exposed to UV light at 1100s, an obviously frequency shift of $\sim 75\text{kHz}$ was observed, and the same phenomenon was observed when the illumination was turned off, the UV light intensity was around 4.5 mW/cm^2 .

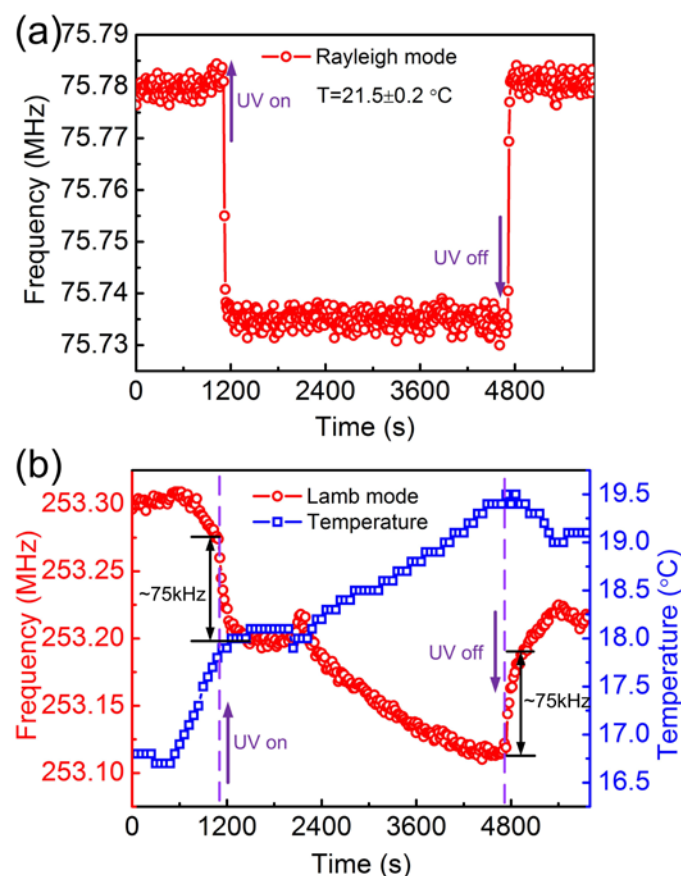


Fig. 9. Long term responses of the dual mode to UV light exposure and temperature: (a) for Rayleigh mode, the temperature was constant, the UV

exposure time is around 1 hour;(b)for Lamb mode, influences of UV light and temperature were measured simultaneously.

These results not only demonstrate that the flexible SAW sensors are repeatable, reproducible and stable, but also imply the PI substrates are very stable as well under a long duration high intensity UV light illumination. Since these SAW devices two wave modes, they can not only sense the UV light intensity using the two wave modes simultaneously, but also can use three variables (resonant frequency, insertion loss and phases angle) for the detection simultaneously, as such it can dramatically improve the accuracy of the detection. Especially considering the change of insertion loss, which is opposite to that reported by others. The tendency of the IL change caused by UV light is also different from that introducing by other parameters, such as temperature, humidity. So it is easy to distinguish the influence of UV light. A dual-mode sensor can also simplify the detection significantly as one of the wave modes can be used for the calibration for other parameters such as the temperature; therefore it requires no additional calibration circuit and test procedure [36].

IV. CONCLUSIONS

Dual-mode flexible ZnO based UV sensors have been fabricated and their performance has been characterized. SAW resonators with Al IDTs were fabricated with good transmission characteristics. These resonators exhibit two well-defined resonant modes with signal amplitudes near 20 dB, corresponding to the Rayleigh wave and Lamb wave respectively, in good agreement with the FEA modeled results. The sensitivity of the Rayleigh and Lamb modes to the UV light are 111.3 and 55.8 ppm/(mW/cm²) respectively, compatible to those obtained from the devices made on rigid substrates. The flexible SAW based UV light sensors exhibited a good repeatability in responding to the cyclic UV light illumination, and the responses of the frequency, phase and insertion loss to UV illumination increase with the increase in light intensity, showing good linearity. This research has demonstrated that not only the dual-mode waves can be used for detecting UV-light simultaneously, but also three transmission variables of the devices can be used for the same purpose, therefore the dual-mode flexible SAW sensors can greatly enhance the sensing accuracy, and reduce the complexity for the calibration. The excellent property of these SAW resonators demonstrated their great potential for applications in flexible electronics, sensors and micro-systems.

REFERENCES

- [1] J.A. Rogers, T. Someya and Y.G. Huang, "Materials and Mechanics for Stretchable Electronics," *Science*, vol. 327, pp.1603-1607, 2010.
- [2] C. Sire, F.S. Lepilliet, J.W. Seo, M.C. Hersam, G. Dambriane, H. Happy and V. Derycke, "Flexible Gigahertz Transistors Derived from Solution-Based Single-Layer Graphene," *Nano.Lett.*, vol. 12, no. 3, pp. 1184-1188, 2012.
- [3] L. Sun, G.X. Qin, H. Huang, H. Zhou, N. Behdad, W.D. Zhou and Z.D. Ma, "Flexible high-frequency microwave inductors and capacitors integrated on a polyethylene terephthalate substrate," *Appl. Phys. Lett.*, vol. 96, no. 1, p. 013509, 2010.
- [4] H. C. Ko, M. P. Stoykovich, J. Z. Song, V. Malyarchuk, W. M. Choi, C. J. Yu, J. B. Geddes, J. L. Xiao, S. D. Wang, Y. G. Huang and J. A. Rogers,

- “A hemispherical electronic eye camera based on compressible silicon optoelectronics,” *Nature*, vol. 454, pp. 748-753, 2008.
- [5] S. Kim, H. Y. Jeong, S. K. Kim, S.Y. Choi and K. J. Lee, “Flexible Memristive Memory Array on Plastic Substrates,” *Nano. Lett.*, vol. 11, no. 12, pp. 5438–5422, 2011.
- [6] K.I. Park, M. Lee, Y. Liu, S. Moon, G.T. Hwang, G. Zhu, J. E. Kim, S. O. Kim, D. K. Kim, Z. L. Wang and K. J. Lee, “Flexible Nanocomposite Generator Made of BaTiO₃ Nanoparticles and Graphitic Carbons,” *Adv. Mater.*, vol. 24, no. 22, pp. 2999-3004, 2012.
- [7] W.C.Lai, J.T.Chen and Y.Y.Yang, “ZnO-SiO₂ solar-blind photodetectors on flexible polyethersulfone substrate with organosilicon buffer layer,” *Appl. Phys. Lett.*, vol. 102, no. 19, p.191115, 2013.
- [8] B. Liu, Z.R. Wang, Y. Dong, Y.G. Zhu, Y. Gong, S.H. Ran, Z. Liu, J. Xu, Z. Xie, D. Chen and G.Z. Shen, “ZnO-nanoparticle-assembled cloth for flexible photodetectors and recyclable photocatalysts,” *J. Mater. Chem.*, vol. 22, pp. 9379-9384, 2012.
- [9] H. Jin, J. Zhou, X.L. He, W.B. Wang, H.W. Guo, S.R. Dong, Y. Xu, D.M. Wang, J. Geng, J.K. Luo and W.I. Milne, “Flexible surface acoustic wave resonators built on disposable plastic film for electronics and lab-on-a-chip applications,” *Sci. Report.*, vol. 3, p. 2140, 2013.
- [10] X.L. He, D.J. Li, J. Zhou, W.B. Wang, W.P. Xuan, S.R. Dong, H. Jin and J.K. Luo, (2013, Jul). “Flexible surface acoustic wave humidity sensors,” *J. Mater. Chem. C.*, vol. 1, pp.6210-6215, 2013.
- [11] V. Chivukula, D. Ciplys, M. Shur and P. Dutta, “ZnO nanoparticle surface acoustic wave UV sensor,” *Appl. Phys. Lett.*, vol. 96, no. 23, p. 233512, 2010.
- [12] P. Sharma and K. Sreenivas, “Highly sensitive ultraviolet detector based on ZnO/LiNbO₃ hybrid surface acoustic wave filter,” *Appl. Phys. Lett.*, vol. 83, no. 17, p.3617, 2003.
- [13] T.T. Wu, W.S. Wang, T.H. Chou and Y.Y. Chen, “Ultraviolet detector based on a surface acoustic wave oscillator system with ZnO-nanostructure sensing material,” *J. Acoust. Soc. America.*, vol. 123, no. 5, pp. 3377-3377, 2008.
- [14] C.L. Wei, Y.C. Chen, C. C. Cheng, K.S. Kao, D.L. Cheng, P.S. Cheng, “Highly sensitive ultraviolet detector using a ZnO/Si layered SAW oscillator,” *Thin Solid Films*, vol. 518, no. 11, pp. 3059-3062, 2010.
- [15] H.F. Pang, Y.Q. Fu, Z.J. Li, Y.F. Li, J.Y. Ma, F. Placido, A. J. Walton and X.T. Zu, “Love mode surface acoustic wave ultraviolet sensor using ZnO films deposited on 36° Y-cut LiTaO₃,” *Sens. & Actuat. A.*, vol. 193, pp. 87-94, 2013.
- [16] W. S. Wang and T. T. Wu, “A micromachined ZnO/Si₃N₄ Lamb wave device for ultraviolet sensing application,” *IEEE Freq. Cont. Symp.*, pp.493-498, Jun. 2010.
- [17] Datasheet of Dupont Kapton, (2013, Apr). [Online]. Available: http://www2.dupont.com/Kapton/en_US/assets/downloads/pdf/summary_ofprop.pdf.
- [18] J. Zhou, X.L. He, H. Jin, W.B. Wang, B. Feng, S.R. Dong, D.M. Wang, G.Y. Zou, and J. K. Luo, “Crystalline structure effect on the performance of flexible ZnO/polyimide surface acoustic wave devices,” *J. Appl. Phys.*, vol. 114, no. 4, p. 044502, 2013.
- [19] H. Kind, H.Q. Yan, B. Messer, M. Law and P.D. Yang, “Nanowire ultraviolet photodetectors and optical switch,” *Adv. Mater.*, vol. 14, no. 2, pp.158-160, 2002.
- [20] D.T. Phan and G.S. Chung, “Characteristics of SAW UV sensors based on a ZnO/Si structure using third harmonic mode,” *Curr. Appl. Phys.*, vol. 12, no. 1, pp. 210-213, 2012.
- [21] C.A. Johnsen, T.L. Bagwell, J.L. Henderson and R.C. Bray, “Polyimide as an acoustic absorber for high frequency saw applications,” in *Proc. IEEE Ultrason. Symp.*, Oct. 1988, vol. 1, pp. 279-284.
- [22] W.C. Qian, A. Venama, “An acoustic absorption film for SAW devices,” *Sens. & Actuat. A.*, vol. 26, nos. 1-3, pp. 535-539, 1991.
- [23] IEEE Standard on Piezoelectricity, ANSI/IEEE Standard 176-1987, 1988.
- [24] C. K. Campbell, *Surface acoustic wave devices for mobile and wireless communications*. New York, NY, USA: Academic Press, 1998.
- [25] L. L. Brizoual, O. Elmazria, F. Sarry, M. E. Hakiki, A. Talbi, P. Alnot, “High frequency SAW devices based on third harmonic generation,” *Ultrasonics*, vol. 45, nos. 1-4, pp. 100-103, 2006.
- [26] L. L. Brizoual, F. Sarry, O. Elmazria, P. Alnot, S. Ballandras and T. Pastureaud, “GHz Frequency ZnO/Si SAW Device,” *IEEE Tran. Ultrason. Ferroelectr. Freq. Control*. Vol. 55, no. 2, pp. 442–450, Feb. 2008.
- [27] L.W. Lai, C.T.Lee, “Investigation of optical and electrical properties of ZnO thin films,” *Mater. Chem. & Phys.*, vol. 110, nos. 2-3, 393–396, 2008.
- [28] A. Wixforth, J. Scriba, M. Wassermeier, and J. P. Kotthaus, “Surface acoustic waves on GaAs/Al_xGa_{1-x}As heterostructures,” *Phys. Rev. B*. vol. 40, no. 11, pp. 7874-7887, 1989.
- [29] J. Pedrós, F. Calle, R. Cuerdo, J. Grajal, and Z. Bougrioua, “Voltage tunable surface acoustic wave phase shifter on AlGaIn/GaN,” *Appl. Phys. Lett.* vol. 96, no. 12. P. 123505, 2010.
- [30] N. W. Emanetoglu, J. Zhu, Y. Chen, J. Zhong, Y.M. Chen, and Y.C. Lu, “Surface acoustic wave ultraviolet photodetectors using epitaxial ZnO multilayers grown on r-plane sapphire,” *Appl. Phys. Lett.*, vol. 85, no. 17, pp. 3702-3704, 2004.
- [31] T.T. Wu, W.S. Wang, T.H. Chou and Y.Y. Chen, “A ZnO nanorod-based SAW oscillator system for ultraviolet detection,” *Nanotechnol.*, vol.20, no. 13, p.135503, 2009.
- [32] X. Qiu, J. Zhu, J. Oiler, C. Yu, Z. Wang and H. Yu, “Film bulk acoustic-wave resonator based ultraviolet sensor,” *Appl. Phys. Lett.*, vol. 94, no. 15, p. 151917, 2009.
- [33] R.B. Peterson, C.L. Fields and B. A. Gregg, “Epitaxial chemical deposition of ZnO nanocolumns from NaOH,” *Langmuir.*, vol. 20, no. 12, pp. 5114-5118, 2004.
- [34] C.C. Wu, D. S. Wu, P.R. Lin, T.N. Chen and R.H. Horng, “Effects of Growth Conditions on Structural Properties of ZnO Nanostructures on Sapphire Substrate by Metal-Organic Chemical Vapor Deposition,” *Nanoscale. Res. Lett.* vol. 4, no. 4, pp. 377-384, 2009.
- [35] D. Singh, A.A. Narasimulu, L. Garcia-Gancedo, Y.Q. Fu, T. Hasan, S.S. Lin, J. Geng, G. Shao and J.K. Luo, “New generation ZnO nanorod films by chemical solution deposition for planar device applications,” *Nanotechnol.*, vol. 24, no. 27, p. 275601, 2013.
- [36] X.L. He, L. García-Gancedo, P.C. Jin, J. Zhou, W.B. Wang, S.R. Dong, J.K. Luo A. Flewitt and W.I. Milne, “Film bulk acoustic resonator pressure sensor with self temperature reference,” *J. Micromech. Microeng.*, vol. 22, no. 12, p. 125005, 2012.



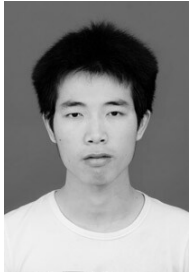
Xing-Li He received the B.S. degree in Microelectronics from Xidian University, Xi'an, China in 2010. Currently, he is a Ph.D. candidate in the Institute of Microelectronics and Optoelectronics, department of information science and engineering, Zhejiang University, Hangzhou, China. His research interests include acoustic resonator, MEMS sensor and lab on a chip system.



Jian Zhou received the B.S. degree in Electronic Science and Technology degrees from Hunan University, China, in 2010. Now he is the Ph.D candidate of physics electronics, in Information Science & Electronic Engineering, Zhejiang University, China. His current research interests include flexible piezoelectric film, flexible SAW device and transparent SAW and FBAR device.

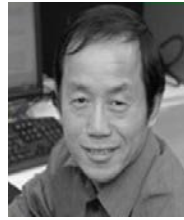


Wen-Bo Wang received the B.Eng degree in Microelectronics from Zhejiang University, Hangzhou, Zhejiang, China, in 2011. Since 2011, He has been a Ph.D. candidate in MEMS group, Institute of Microelectronics and Optoelectronics, Department of Information Science and Engineering, Zhejiang University, Hangzhou, Zhejiang, China. His research interests include surface acoustic wave sensor and actuator, microfluidic device and lab on a chip system.



Wei-Peng Xuan received the B.S. degree in Electronic Science and Technology from Hunan University, Changsha, China in 2012. Currently, he is pursuing the Ph.D degree in Microelectronics and Solid-state Electronics in Zhejiang University. His current research is wireless SAW sensor and SAW based gas sensors.

academic visitor supported by the EPSRC project of U.K., developing FBAR model and its application on biosensor. He became an associate professor of MEMS at Zhejiang University, P.R. China, in 2012. He is the inventor in 4 patents and has published over 30 papers in peer reviewed journals and international conference proceedings



Ji-Kui Luo received his Ph.D. from the University of Hokkaido, Japan in 1989. He worked in Cardiff University as a research fellow, in Newport Wafer Fab. Ltd., Philips Semiconductor Co. and Cavendish Kinetics Ltd. as an engineer,

senior engineer and manager, and then in Cambridge University as a senior researcher from 2004. From January 2007, he became a Professor in MEMS at the Centre for Material Research and Innovation (CMRI), University of Bolton. His current research interests focus on microsystems and sensors for biotechnology and healthcare applications, and third generation thin film solar cells using novel low cost materials.



Hao Jin received his PhD degree from Zhejiang University, P.R. China in 2006. After graduation, he worked as a RF engineer at Semiconductor Manufacturing International Corporation, P.R. China, to develop the high accurate RF model of CMOS devices. From 2007, he worked as a faculty at Zhejiang University, P.R. China, on the magnetron sputtering processes and RF MEMS devices. In

2011, he visited the University of Manchester, U.K. as an